Understanding effects of climate and socio-economic changes on water allocation adaptation needs in an Indian Himalayan basin

Quan V. Dau and Adebayo J. Adeloye*

Institute for Infrastructure and Environment, Heriot-Watt University, Edinburgh, EH14 4AS, UK

Abstract: Changes to climate in recent decades have resulted in huge losses of glaciers, and alteration of the hydrologic balance in Northern region of India. Simultaneously, rapid and continuous population growth together with economic development are combining to increase water demands. Understanding this complex interplay is important if effective adaptation strategies for the water security repercussions are to be developed. This study has investigated the impacts of climate and socio-economic changes on water resources in the Beas-Sutlej River Basin of the Indian Himalaya. To project future meteorological conditions for hydrologic analysis, the GFDL-CM3 model was used, forced with the Representative Concentration Pathway (RCP) 8.5 scenario. Shared Socio-economic Pathway SSP 1 was also used to project the future population and land use situations. These projected hydrologic and socio-economic scenarios were used to force a validated Water Evaluation And Planning (WEAP) model of the basin for the purpose of assessing the sectoral water allocations. The results showed increasing runoff during the pre-monsoon and monsoon seasons, principally as the respective consequences of increased glaciers melting and heavier monsoon rainfall. The finding also indicates that irrigation water demand will reduce by between 8 to 13% in Punjab and by between 1 to 9% in Haryana, principally due to the conversion of agricultural land to urban centres. The situation was reversed for the State of Rajasthan where an increase in irrigation water demand about 14% was projected. While this has only utilised a single RCP and GCM, the outcomes will be useful for the Bhakra and Beas Management Board (BBMB) in developing adaptation strategies for any future water shortages that may occur in the basin.

Keywords: *Climate change; socio-economic change; WEAP; irrigation water demand; hydrology*

1. Introduction

The Himalayas are an essential freshwater source for 1.9 billion people across South Asia river basins. In India alone, more than 900 million people are relying on its water resources for agriculture, domestic, and industrial uses. However, evidence in the last few decades have confirmed that demand for water in India has dramatically increased due to rapid population and socio-economic growths whilst the quality and quantity of the available water resources are declining due to the impacts of climate and other environmental changes. Shivakoti *et al.* (2016) believe that the scarcity of water, energy and food will probably increase by between 40% to 50% by 2050 in Asia. For example, India is already the world's second most populous country, but its population is projected to rise to more than 1.5 billion by 2030 and 1.7 billion

* Corresponding Author: Professor Adebayo J. Adeloye, Heriot-Watt University, Edinburgh, EH14 4AS, United Kingdom. E-mail: a.j.adeloye@hw.ac.uk

by 2050 (UN, 2019). Such a phenomenal growth in population will obviously result in high water demand, stress natural resources, and ultimately stifle regional economic development.

Additionally, climate change has also been proven to be a major threat to the security of freshwater resources in the Himalayan region. According to the Intergovernmental Panel on Climate Change (IPCC), India could face the harshest effects of global warming, including high levels of inequality and poverty (IPCC, 2018). A major aspect of this is the rising temperature which has been shown to increase by 0.74°C in the past 10 decades in the Himalaya (Du *et al.*, 2004) and more significant rises of between 2.36ºC to 5.51ºC are projected for the end of the Century (Chaturvedi *et al.*, 2014). Increasing temperatures will result in drastic glaciers losses and alteration to the hydrologic balance. The fact is the Himalayan glaciers are retreating rapidly year by year. For instance, average thinning rate is estimated to be 0.3 to 1 m/year (Dyurgerov & Meier, 2005), with the corresponding loss rising by an estimated 6.6 ± 1 Gt/year (Kulkarni & Karyakarte, 2014). Glacier and seasonal snow melt currently contributes about 70% of the runoff to the Indus, Ganges, and Kabul rivers (Barnett *et al.*, 2005; Kattelmann, 1987). Within the Indus basin specifically, the contribution is 59% of runoff in the Sutlej River at the Bhakra Dam, and 35% to the Beas River at Pandoh Dam (Kumar *et al.*, 2007).

The Himalayan freshwater resources are very vital for sustaining agricultural production in the Indus basin by supporting large scale irrigation projects in the States of Punjab, Rajasthan, and Haryana. According to the Punjab Reorganisation Act 1966, approximately of 17.28 BCM (billion cubic meter) water from the Bhakra dam, 21.18 BCM from the Pong dam, and 1.369 BCM from the Ravi tributary was used for irrigation between 1921 and 1960. This dependence on the basin’s water resources has since grown significantly due to the rising population and climatic change and is expected to grow even further based on the future projections of these variables. It is therefore important to fully understand the impacts of these factors- climate, population and their complex interlay- because without this, it will be difficult if not impossible to develop appropriate adaptation measures.

2. Study Area and Methods

Study Area

The Beas-Sutlej river basin (see Fig.1) has a total area of 76,400 km^2, of which 34,100 km^2 in the Himachal Pradesh and Punjab, and 42,300 km^2 is in the Tibet Autonomous region, China (Momblanch *et al.,* 2019). The Beas River originates from the upper part of the Himalayas and is wholly within India, whereas the Sutlej starts near Lake Rakhastal in the Tibetan plateau outside India and then flows through Himalayan gorges before merging with the Beas at a location near the Punjab State. There are two main water resources facilities in the basin- the Pong dam on the Beas River and Bhakra dam on the Sutlej whose associated reservoirs serve large scale irrigation projects, generate hydro-electric power and provide flood relief. Measured runoff at the inlets of the reservoirs as well as at four other sites – Thalout, Namgia, Nadaun, and Kasol – were available for the study.

According to the India Ministry of Agriculture, gross irrigated areas are 7.442 million hectares (M-ha) in Punjab, 5.446 M-ha in Haryana and 8.09 M-ha in Rajasthan (DAC, 2018). For crops production, Punjab produces majorly wheat, rice, and cotton. In Haryana, the *Kharif* crops are sugarcane, wheat, groundnut, maize, and paddy, while, barley and cotton are grown in the *Rabi* season. Similarly, the *Kharif* crops in Rajasthan are bajra, pulses, jowar, maize, and groundnut, while the *Rabi* crops consist of barley, wheat, gram, and oil seeds (DAC, 2018).

The gross water requirements at Punjab is estimated 61.5 BCM, against the current availability of 36.6 BCM, with 15.2 BCM of this being surface water (Kaur *et al.*, 2010). For Haryana, the present water availability is around 17 BCM, but this is projected to increase to 45 BCM by 2045 (Rawat *et al.*, 2018). Rajasthan also relies on both surface and groundwater sources for irrigation (Gupta *et al.*, 2015) but there is a current deficit of 9 BCM (Singh *et al.*, 2013).

Rainfall mostly occurs in the monsoon season between July and late September. The average annual rainfall is about 1,800 mm at the Beas catchment and 1,200 mm at the Sutlej catchment. Temperature lapse rate in the Western Himalayas ranges between 0.6 and 0.74^{o}C/100 m (Jain *et al.*, 2008), producing mean annual temperature of between -22.2 and 23.3^{o}C depending on the altitude (Momblanch *et al.*, 2019). In the Tibetan Plateau where the Sutlej originates, climate is both drier and warmer in comparison to the Himalayan watershed (You *et al.*, 2008). For example, the average annual rainfall in the Tibetan Plateau (Sawatpru & Konyai) is about 250 mm, while the annual minimum temperature is approximately -10 to 4^{o}C and annual maximum temperature is between 5 and 20^{o}C (Ding *et al.*, 2018), which has increased by about 1.8^{o}C since the 1960s (Wang *et al.*, 2017). Snow meltwater has recently shown an increasing rate in the Himalayan during the summer due to the rising temperatures.

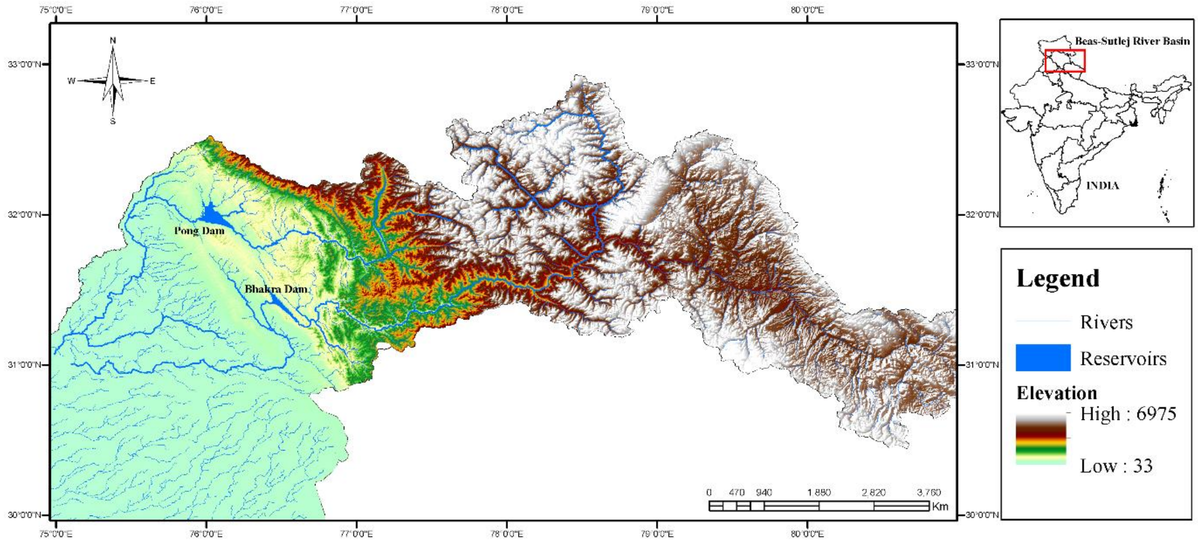

Fig. 1 The Beas-Sutlej river basin, India

Methodology

Data collection

Monthly precipitation and temperature data were obtained from the Bhakra and Beas Management Board (BBMB) for the period of 1990 to 2007. Humidity and wind speed data were derived from the NASA Science Mission Directorate's Satellite (NASA, 2018). Monthly streamflow for the four gauged sites and reservoir inlets and other reservoir information such as bathymetric data and releases were obtained from the BBMB and various other sources. For future climate projection relative to the current condition, outputs from a coupled climate model developed at the NOAA Geophysical Fluid Dynamics Laboratory (GFDL), Climate Model version 3 (CM3) was used. The CM3, with 2^{o} latitude x 2.5^{o} longitude grid scale, builds on the extensive experience garnered from the earlier GFDL Climate Model version 2.1 (CM2.1) (Delworth *et al.*, 2006).

For describing the spatial variability of vegetation and land use, land cover maps (version 2.0.7) at 300 m spatial resolution developed by the European Space Agency Climate Change Initiative (ESA-CCI) for the years of 2000, 2005, and 2010 were used (UCLouvain, 2017). The Land and Water Development Division – FAO soil type map was also used to provide an overview of the soil distribution in respect of soil moisture conditions of irrigation lands. Other physical datasets such as elevation, slope, roads, and river were reanalysed using the ASTER Global Digital Elevation Model (DEM) data at 30 m resolution.

Population is an important driver for understanding potential future interactions between climate and human society change. In this study, projected population for 10 year intervals time-slice from 2010 to 2100 obtained from the Climate and Global Dynamics Laboratory (CGD) - part of the National Center for Atmospheric Research (NCAR), containing of 1/8-degree resolution downscaled by (Jones & O'Neill, 2016) and 1-km grid cells re-downscaled by Gao (2017) was used for quantifying the domestic water consumptions.

Downscaling climate model with Delta Change approach

CM3 projected rainfall and temperature data for RCP 8.5 scenario were downscaled using the Delta Change approach proposed by (Lenderink *et al.*, 2007).

For precipitation, the Delta Change is given by:

$$\Delta P_m^{GFDL-CM3} = \frac{P_m^{GFDL-CM3,F}}{P_m^{GFDL-CM3,H}} \quad (1a)$$

And for temperature, the Delta Change is given by:

$$\Delta T_m^{GFDL-CM3} = T_m^{GFDL-CM3,F} - T_m^{GFDL-CM3,H} \quad (1b)$$

where, P is precipitation, T is temperature, F refers to a future time slice, H refers to the historical/baseline period, m refer to specific month.

Once the Delta Changes have been obtained, they were then applied to the high-resolution (5 km x 5 km) climate hindcast (or baseline) developed with Weather Research Forecasting (WRF) dynamical downscaling model to provide the corresponding high-resolution future climate projection for month *m* and year *y* as:

$$P_{m,y}^{WRF,F} = P_{m,y}^{WRF,H} \times \Delta P_m^{GFDL-CM3} \quad (2a)$$

$$T_{m,y}^{WRF,F} = T_{m,y}^{WRF,H} + \Delta T_m^{GFDL-CM3} \quad (2b)$$

Using equations 2a and 2b, future projections with respect to the mid-century (2033 – 2050) and end-century (2083 – 2100) were then developed.

Projected land use change with Markov Chain analysis

Markov Chain analysis is a dynamic processes based on Markovian random process, which has been used extensively for projecting land cover change (Fathizad *et al.*, 2015; Gibson *et al.*, 2018). The method requires the transition probability matrix, which gives probability of land cover changes from one period to another. Once the transition probability matrix is known, the state of the system after one transition becomes (Hamad *et al.*, 2018; Liping *et al.*, 2018; Marko *et al.*, 2016):

$$S_{(t+1)} = \tau \times S_t \tag{3}$$

where, S_t is the state of the system at time t, S_{t+1} is the state at time $t+1$, i.e. after a single transition and τ is the transition probability matrix given by:

$$\tau = \begin{vmatrix} \tau_{11} & \tau_{12} & \cdots & \tau_{1n} \\ \tau_{21} & \tau_{22} & \cdots & \tau_{2n} \\ \cdots & \cdots & \cdots & \cdots \\ \tau_{n1} & \tau_{n2} & \cdots & \tau_{nn} \end{vmatrix} \tag{3a}$$

$$\sum_{j=1}^{n} \tau_{ij} = 1 \ ; i, j = 1, 2, \ldots n \tag{3b}$$

$$0 \le \tau_{ij} \le 1 \tag{3c}$$

The elements τ_{ij} of τ represent the probability of the system transitioning from state (land use type) i to state (land use type) j and n is the total number of land use types. When $i = j$, the system is persistent, i.e. no transition has taken place; otherwise there is transition. Thus, the main diagonal elements of matrix τ contain the persistent probabilities.

The main task for the land use cover change projections therefore is the determination of the transition probability matrix. One popular approach that has been used is to model the relationship between land use patterns and those factors that have been known to influence them. For example, it has been noted that land use is dependent on various explanatory variables such as such as elevation, slope, distance to urban, rivers, roads, population, and Gross Domestic Product (GDP), which can serve as factors for explaining how potential transition of land use change respond to socio-economic changes. Given that the relationship may be complex and difficult to express in closed mathematical forms, a data-driven, multi-layer perceptron artificial neural network (ANN) was used to model the relation between the explanatory variables as inputs and the transition probabilities as output. Once trained and validated, the resulting model can be used to obtain the transition probabilities for future time-slices once projections of the explanatory variables are known.

The use of ANN for modelling environmental systems is well known and no useful purpose will be served by repeating its details here. Performance of the Multiplayer Perceptron (MLP) during training is measured by the accuracy rate, i.e. the difference between prediction and observation of both transition and persistence probabilities. For model validation, the Kappa statistic was used for assessing the agreement between two categorical images, where each cell in maps has a multinomial distribution among any number of categories. Details of the Kappa statistic are available elsewhere e.g. (Monserud & Leemans, 1992; Pontius, 2000, 2002). Agreement in cells of compared maps use the information of location and quantity, and the Kappa index of agreement is obtained using:

$$Kappa = \frac{(P_0 - P_c)}{(P_p - P_c)} \tag{4}$$

where, P_0 is the observed proportion correct; P_c is the expected proportion correct due to chance; P_p is the proportion correct when classification is perfect for both location and quantity.

Land cover maps for the years 2000 and 2005 were used for the training and testing and that for 2010 was used for validation.

WEAP allocation modelling

The Water Evaluation and Planning (WEAP) model developed by the Stockholm Environment Institute (SEI) (Sieber & Purkey, 2011) has been widely used worldwide in many regional water allocation problems, e.g. (Dau *et al.*, 2018; Kou *et al.*, 2018; Momblanch *et al.*, 2019).

A schematic system of the WEAP model for the Beas-Sutlej River Basin is presented in Fig. 2. Catchments were defined based on the availability of river system within the basin, and then subdivided into different elevation bands (roughly 600 m). Total runoff was calculated using two compartments of the soil water balance (Yates *et al.*, 2005): the upper compartment that simulates surface runoff when forced with rainfall and evapotranspiration; and the lower compartment that simulates baseflow. Fuller details of the rainfall-runoff modelling of WEAP are available elsewhere (Dehghanipour *et al.*, 2019; Rajeevan & Mishra, 2020; Sridharan *et al.*, 2019).

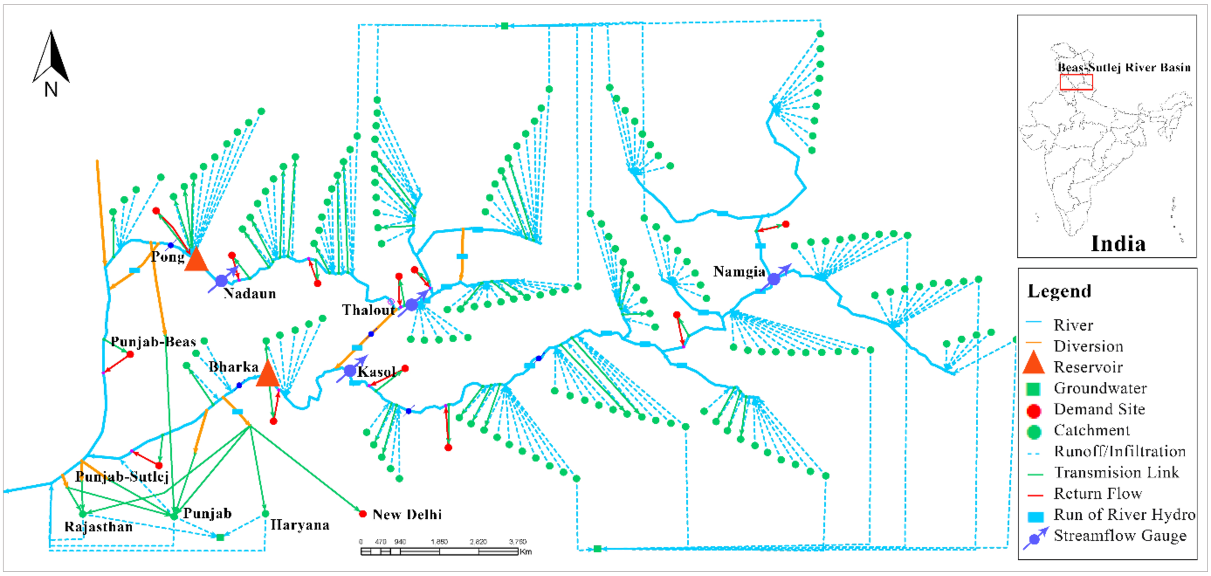

Fig. 2 Schematic of WEAP model for the Beas-Sutlej River Basin, India

According to WaterAid-India (2005), daily water consumption per capita in India is estimated to be 40 litters for rural areas and 135 litters in urban areas. As shown in Fig. 2, the basin has a number of domestic water demand centres relying on its water resources. For example, New Delhi takes some of its water supply from the basin and any significant growth in Delhi population in the future will negatively impact the reliability of the domestic sector allocation. The impact of this on the overall system reliability, however, will be minimal given the dominance of irrigation water allocation over all other sectors.

As for irrigation demand, WEAP uses the MABIA (MAitrise des Besoins d'Irrigation en Agriculture) (Agarwal *et al.*, 2019; Sieber & Purkey, 2011) method to determine actual evapotranspiration or irrigation demands in the Punjab, Rajasthan, and Haryana states. MABIA uses the "dual K_c" method to determine the actual evapotranspiration from the reference crop evapotranspiration.

The performance of the reservoirs in meeting the various demands from their allocations was characterised using the usual indices (Adeloye & Dau, 2019): time-reliability (R_t), ; volume-reliability (R_v),; resilience (φ), and vulnerability (η) as follows:.

$$R_t = \frac{N_s}{N};\ 0 < R_t \leq 1 \tag{5}$$

$$R_v = 1 - \frac{\sum_{t=1}^{N}(D_t - D'_t)}{\sum_{i=1}^{N} D_t}; \ (0 < R_v \leq 1) \tag{6}$$

$$\varphi = \frac{f_s}{f_d}; \quad f_d \neq 0 \tag{7}$$

$$\eta = \frac{\sum_{t=1}^{f_d}[(D_i - D'_i)/D_i]}{f_d}; \ t \in f_d \tag{8}$$

where, N_s is total number of months out of *N* month that demand was met; f_s and f_d is number of continuous sequences of failure periods and the total duration of the failures, respectively

Scenario testing for future water demand

The scenarios tested are summarised in Table 1 based on climate change (RCP 8.5) and socio-economic change (SSP1). In total four scenarios are considered for mid and end of Century, with the first two involving both land use and socio-economic changes whilst the last two only investigated climate change. This should help to identify the relative significance of the two effects on future water security in the basins.

Table 1. Scenarios testing for the Beas-Sutlej River Basin

Scenarios	SSPs	Mid-century	End-century
Socio-economic and Climate change	SSP1	1-*Mid*-LU-SSP1&RCP	2-*End*-LU-SSP1&RCP
Climate Change only		3-*Mid*-RCP	4-*End*-RCP

Note: *Mid* is mid-century; *End* is end-century; LU is land use change projection

3. Results and Discussions

Climate change assessment on rainfall and runoff

As noted earlier, the delta change approach coupled with WRF dynamically downscaled hindcast was used to downscale the RCP 8.5 GFDL-CM3 model projections from a coarse global scale into watershed level. The resulting annual changes are shown in Fig. 3a and 3b which reveal that mean annual rainfall will decrease by 3% in the mid-century and increase by 5% in the end-century in comparison to the baseline period. In addition, mean annual temperature is also projected to increase considerably by about 2.4 to 6.2^{o}C in the future, depending on the elevation band.

The annual changes mask the strong seasonality in the changes as revealed in Fig. 3c and 3d. In general, significantly more monsoon rainfall is projected but the basin will be drier at other seasons.

(a)

(b)

(c)

(d)

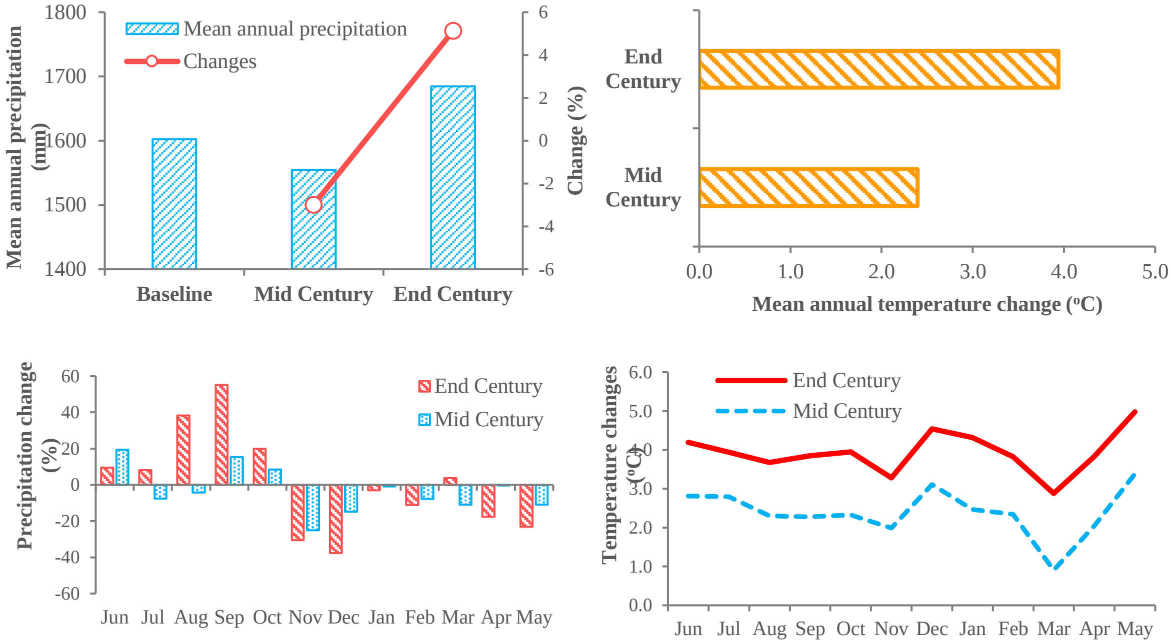

Fig. 3 Mean annual precipitation (a), temperature (b) and changes in monthly precipitation (c) and temperature (d)

Socio-economic projections

Projected population in the future

Fig. 4 shows the projections of population under SSP1. The population will rapidly increase in the mid-century by 45% but thereafter decrease by 15%, both relative to the baseline with implication for the demand centres allocation. For example, New Delhi population will increase by 72% and 94% in mid- and end-century, respectively. As noted earlier, these are significant population changes; however, when translated to water allocation, this is only about 1 BCM much smaller than the current irrigation demand of 61.5 BCM in Punjab State alone.

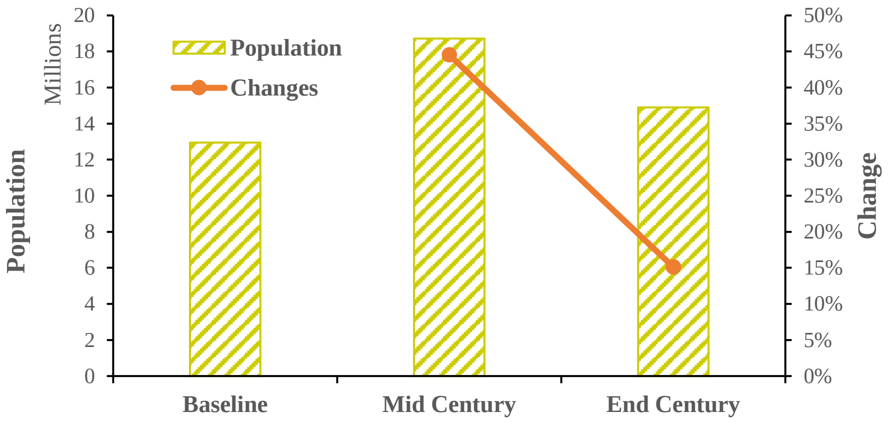

Fig. 4 Projected population under SSP1 in the Beas-Sutlej river basin

Land use change projection

Selection of appropriate explanatory variables is a crucial step for land use change analysis. Seven basic explanatory variables were used in the Beas-Sutlej river basin for land use change projections as listed in Table 2. The correlation of these variables with land use change was determined using Cramer's phi (φ_c) test, which is derived from Pearson's Chi-squared statistic (Cramér, 1946). Classification for each explanatory variable is based on the suggestion by Akoglu (2018), i.e. φ_c > 0.25 is very strong; > 0.15 is strong; > 0.10 is moderate; > 0.05 is weak; and 0 is not meaningful. The obtained φ_c values are presented in Table 2 from which it is clear that most are strongly or very strongly correlated with land use pattern.

Table 2. Potential explanatory variables for land use change projection

No	Explanatory variables	φ_c	Interpretation
1	Elevation	0.3746	Very strong
2	Population 2000	0.2604	Very strong
3	Slope	0.2478	Strong
4	GDP 2000	0.2142	Strong
5	Distance to city	0.1992	Strong
6	Distance to rivers	0.1336	Moderate
7	Distance to roads	0.0896	Weak

The accuracy rate of MLP neural network in modelling the transition probability was very high (> 80%) during both the training and testing stages. The obtained root mean squared errors (*RMSE*) index varied between 0.01 and 0.37, which is very low. Additionally, the performance of the Markov simulation was assessed by comparing the simulated and observed land maps in 2010, i.e. Kappa Indices of Agreement, and this was greater than 96.43%. Table 3 compares the observed and simulated land use for an independent year 2010 which further confirms the high efficacy of the Markov chain model.

Table 3. Observed and simulated land use

Land use types	1995 (Km^2)	2000 (Km^2)	2005 (Km^2)	2010 Observed (Km^2)	2010 Simulated (Km^2)	Errors Km^2	Errors %
Rainfed land	14,410	14,492	14,174	14,022	13,845	-177	-0.1
Irrigated land	85,302	85,218	84,300	83,762	83,406	-356	-0.2
Sparse vegetation	7,761	8,010	7,943	7,843	7,886	43	0.0
Broadleaved evergreen	559	554	563	571	569	-2	-0.0
Broadleaved decidious	4,246	4,399	4,645	4,767	4,853	86	0.1
Needleleaved evergreen	7,888	7,547	7,606	7,712	7,663	-48	-0.0
Needleleaved decidious	24	25	25	25	25	0	0.0
Mixed forest	9	9	9	9	9	0	0.0
Shrub	20,505	20,379	20,139	20,085	19,926	-159	-0.1
Grassland	9,622	9,586	9,504	9,487	9,485	-2	-0.0
Swamp	60	60	61	61	61	0	0.0
Urban	237	285	1,616	2,226	2,864	638	0.4
Bare	5,320	5,351	5,347	5,347	5,347	0	0.0
Water Bodies	577	593	593	591	595	3	0.0

Snow	1,649	1,649	1,649	1,649	1,649	0	0.0

With the Markov chain model satisfactorily validated, it was used to project land use change for 5-year intervals between 2015 and 2100. The mid- and end-century situations are shown in Fig. 5. Fig. 5 suggests that irrigation land will decrease in the Punjab by 15 to 30%, and by 5 to 10% in Haryana. These findings are consistent with the observed trend during 2000 to 2005, where around 31,300 hectares of irrigation land was lost due to conversion of agriculture to urban centres. In contrast, Rajasthan irrigation land is expected to expand by between 12 and 18% in the future compared to the baseline period.

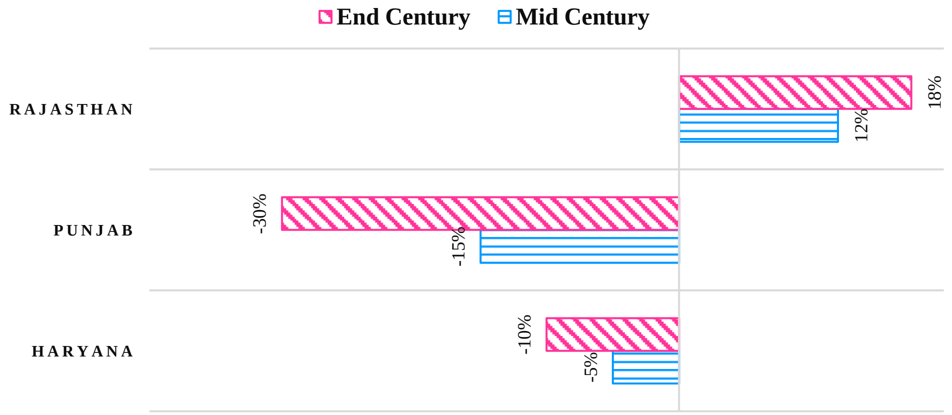

Fig. 5 Land use changes for mid- and end-century

Water demand allocation using the WEAP model

The performance of the rainfall-runoff simulation by WEAP is illustrated in Fig. 6 which compares the measured and simulated flows at the gauged sites in the basin. In general, the performance is good as confirmed by both the Nash-Sutcliffe efficiency criterion (N_{se}) (Nash & Sutcliffe, 1970) and the correlation coefficient (R) during calibration as follows: Thalout (N_{se}= 74%, R = 86%), Namgia (N_{se}= 64%, R = 80%), Namdaun (N_{se}= 80%, R = 90%), Kasol (N_{se}= 62%, R = 81%), Pong (N_{se}= 53%, R = 84%), and Bhakra (N_{se}= 70%, R = 87%). The performance of the model at the reservoir sites during low flow conditions is very good, which is important because the low flows determine the performance of reservoirs in meeting the demand obligations placed on them.

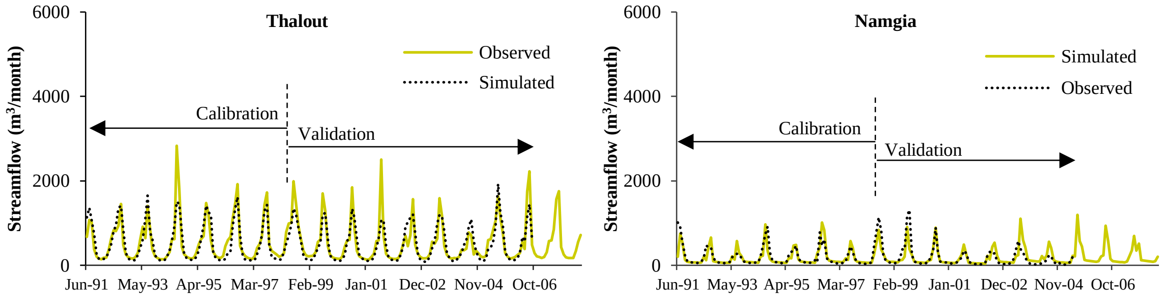

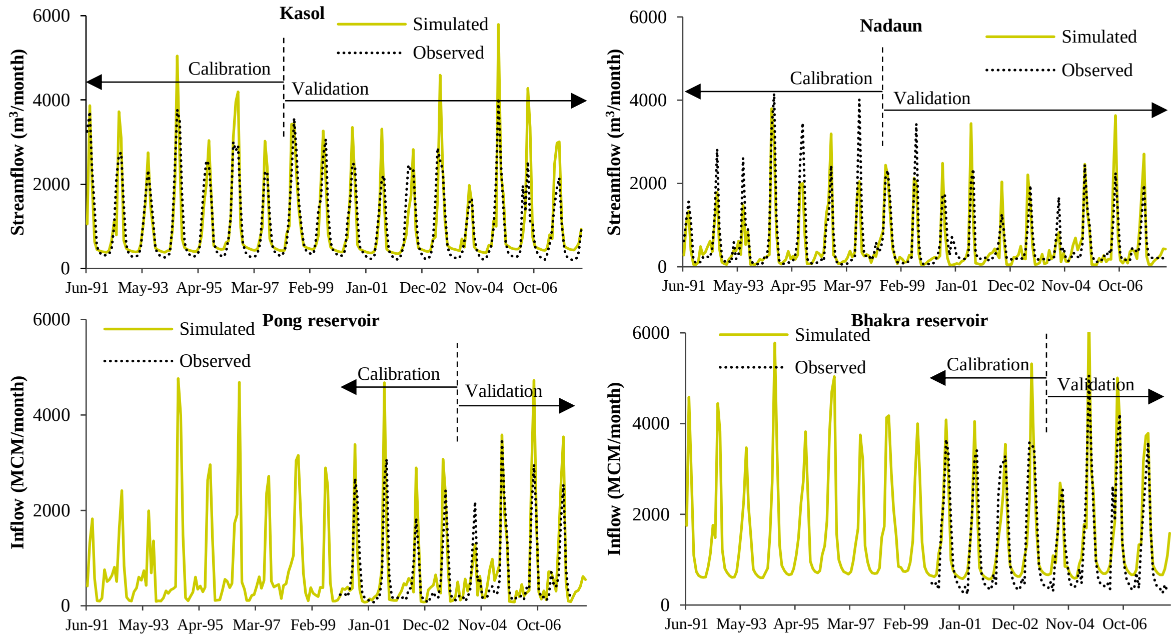

Fig. 6 Simulated and observed monthly streamflow during calibration and validation

The projected irrigation water demands are shown in Fig. 7a and the resulting changes relative to the baseline are shown in Fig. 7b. Under scenarios 1 and 2, irrigation water demand will reduce by about 13% in Punjab, 9% in Haryana, but rise in Rajasthan by about 14% in the end-century (Fig. 7b). These changes agree with the land use changes reported in Fig. 5 in which it was revealed that significant conversion of irrigation lands will take place at both Punjab and Haryana whereas the reverse is projected for the State of Rajasthan. Since irrigation water demand is directly related to the hectarage under cultivation and given only modest changes in the precipitation, it is not at all surprising that the irrigation water demand situations in the three States will be as depicted in Fig. 7. However, for scenarios 3 and 4 which are only concerned with climate change, the projected changes in irrigation water demands are very marginal compared to those recorded for scenarios 1 and 2. This finding suggests that climate change has less impact to irrigation water demand in comparison on the socio-economic change, i.e. land use change.

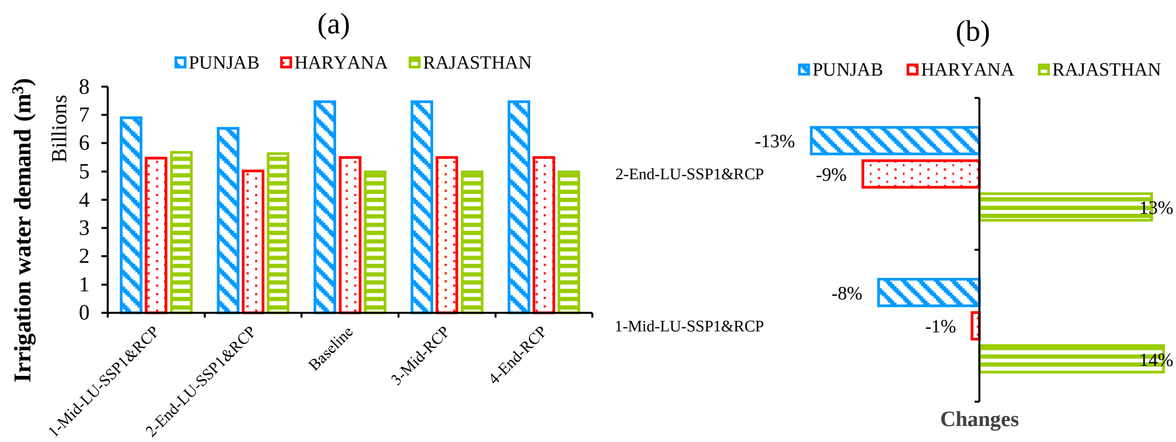

Fig. 7 Water demand for irrigation with different scenarios in the Beas-Sutlej river basin

The performance indices of the water resources systems in meeting the irrigation water demands are shown in Fig. 8. The high reduction in irrigation lands in the Punjab has no doubt translated to much better performance of the water resources systems in satisfying the smaller demand. Thus, the time- and volume-based reliability (89% and 90% respectively) at Punjab in the future exceed those of the baseline (70% and 83% respectively). The same is true for Haryana State, where the time- and volume-based reliability (65% and 89% respectively) in the future also exceed the baseline (42% and 72% respectively). More importantly, the vulnerability which characterises the maximum single period water shortage in Punjab will reduce significantly from 56% (baseline) to 35% (end-century). Similarly, at Haryana, the vulnerability will reduce from 34% to 20%.

Due to expansion of agriculture land in the future, reliability for the irrigation water demand in Rajasthan is expected to reduce from 82% to 75% (time-domain) and for 87% to 84% (volume-domain). At the same time, vulnerability will increase from 25% to 45%.

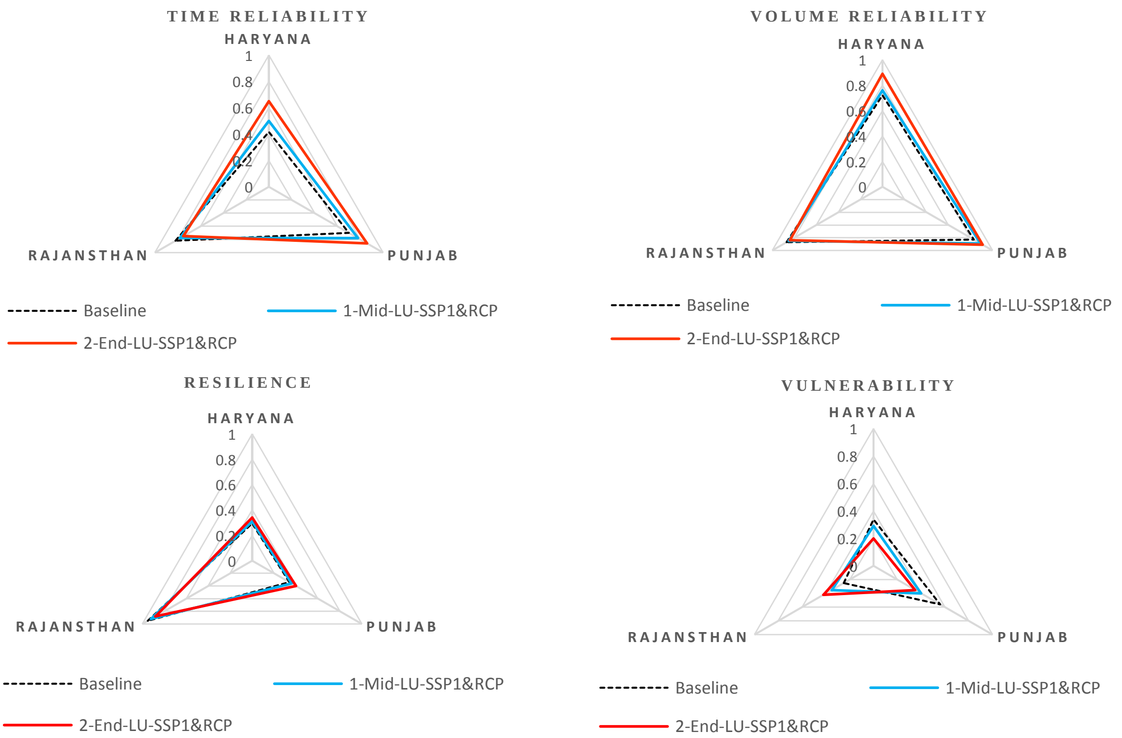

Fig. 8 Performance indices for irrigation water allocation for different scenarios

The performance in relation to hydro-electric power generation at both the Pong and Bhakra reservoirs are shown in Fig. 9. As revealed in the Figure, the hydropower performance will be enhanced significantly at the Pong and Bhakra reservoirs as one would expect from the increased runoff projected for the future and the smaller irrigation water demand both of which will enhance the available head for hydropower generation at both reservoirs. The reliability measured at both the reservoirs reveals an increasing value for all the scenarios in comparison to the baseline. This improvement has been very marked at the Bhakra reservoir, with the time reliability increasing from about 62% to almost 96% depending on the scenario. The impact on the volume reliability is more modest, which is understandable given that it was previously high for the baseline. The trend of the vulnerability is also desirable, with this projected to reduce in the future under most of the scenarios.

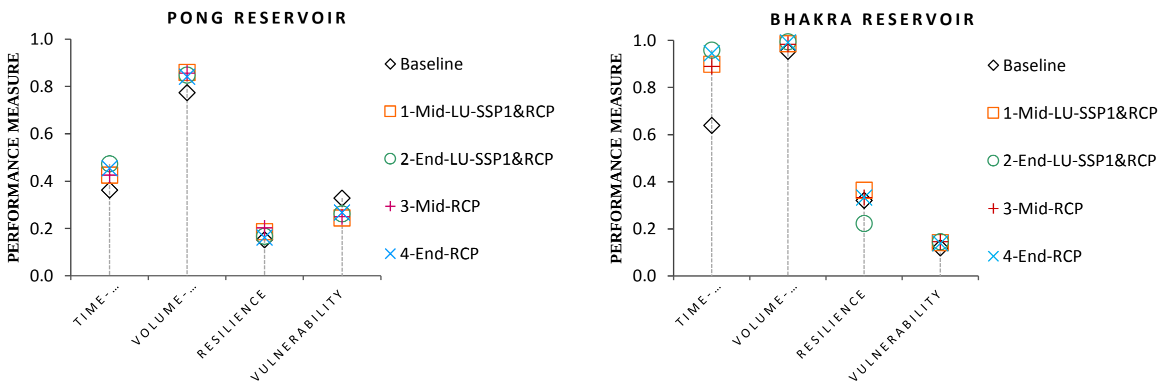

Fig. 9 Performance indices for hydropower generation at the Pong and Bhakra reservoirs for different scenarios

4. Conclusions

Evaluation of the effects of global climate and socio-economic changes on water resources security in the Beas-Sutlej river basin in India Himalaya was carried out. The results reveal that high runoff is likely to occur over the pre-monsoon to monsoon seasons, as consequence of glacier melting associated with rising temperature and the heavy rainfall. Extensive analyses of land use changes suggest large shifts of irrigation lands to urban centres in the downstream States of Punjab and Haryana whereas the opposite occurred in the State of Rajasthan. The effect of these land use changes were significant decreases in irrigation water demands at Punjab (13%) and Haryana (9%), while the requirement at Rajasthan by 14%. However, when the effect of only climate change was considered, the resulting impacts of were much less that when socio-economic changes were included. This shows that climate change has less impacts on irrigation water demand in comparison to the socio-economic changes. Due to high inflows that are expected arrive to at the Pong and Bhakra reservoirs in the future and the reduced allocation to irrigation needs, hydropower generation at the two reservoirs is projected to be enhanced in the future leading to improved performance. All these insights will be useful for planning adaptation strategies for coping with the drivers (climate and socio-economic changes) of water insecurity in the Beas-Sutlej river basin.

Acknowledgements

The work reported here was funded by the UK-NERC (Project NE/N016394/1) – "Sustaining Himalaya Water Resources in a Changing Climate (SusHi-Wat)" – as part of the UK-India Newton-Bhakha Sustainable Water Resources (SWR) thematic Programme.

References

Adeloye, A. J., & Dau, Q. (2019). Hedging as an adaptive measure for climate change induced water shortage at the Pong reservoir in the Indus Basin Beas River, India. *Science of The Total Environment, 687*, 554-566. doi:10.1016/j.scitotenv.2019.06.021

Agarwal, S., Patil, J. P., Goyal, V. C., & Singh, A. (2019). Assessment of water supply-demand using water evaluation and planning (WEAP) model for Ur River watershed, Madhya Pradesh, India. *Journal of The Institution of Engineers (India): Series A, 100*, 21-32.

Akoglu, H. (2018). User's guide to correlation coefficients. *Turkish Journal of Emergency Medicine, 18*(3), 91-93. doi:10.1016/j.tjem.2018.08.001

Barnett, T. P., Adam, J. C., & Lettenmaier, D. P. (2005). Potential impacts of a warming climate on water availability in snow-dominated regions. *Nature, 438*(7066), 303-309. doi:10.1038/nature04141

BBMB. (2018). Bhakra Beas Management Board, An ISO 9001, 14001 Certified Board. Retrieved from http://210.212.64.190/BBMB

Chaturvedi, R. K., Kulkarni, A., Karyakarte, Y., Joshi, J., & Bala, G. (2014). Glacial mass balance changes in the Karakoram and Himalaya based on CMIP5 multi-model climate projections. *Climatic Change, 123*(2), 315-328. doi:10.1007/s10584-013-1052-5

Cramér, H. (1946). *Mathematical Methods of Statistics (PMS-9)* (Vol. 9). Princeton: Princeton University Press.

DAC. (2018). State farmer guide. Retrieved from http://farmech.dac.gov.in

Dau, Q. V., Kuntiyawichai, K., & Suryadi, F. X. (2018). Drought severity assessment in thelower Nam Phong River Basin, Thailand. *Songklanakarin J. Sci. Technol., 40*(4), 985-992. doi:10.14456/sjst-psu.2018.99

Dehghanipour, A. H., Zahabiyoun, B., Schoups, G., & Babazadeh, H. (2019). A WEAP-MODFLOW surface water-groundwater model for the irrigated Miyandoab plain, Urmia lake basin, Iran: Multi-objective calibration and quantification of historical drought impacts. *Agricultural Water Management, 223*, 105704. doi:10.1016/j.agwat.2019.105704

Delworth, T. L., Broccoli, A. J., Rosati, A., Stouffer, R. J., Balaji, V., Beesley, J. A., . . . Zhang, R. (2006). GFDL's CM2 global coupled climate models. Part I: Formulation and simulation Characteristics. *19*(5), 643-674. doi:10.1175/jcli3629.1

Ding, J., Cuo, L., Zhang, Y., & Zhu, F. (2018). Monthly and annual temperature extremes and their changes on the Tibetan Plateau and its surroundings during 1963–2015. *Scientific Reports, 8*(1), 11860. doi:10.1038/s41598-018-30320-0

Du, M., Kawashima, S., Yonemura, S., Zhang, X., & Chen, S. (2004). Mutual influence between human activities and climate change in the Tibetan Plateau during recent years. *Global and Planetary Change, 41*(3), 241-249. doi:10.1016/j.gloplacha.2004.01.010

Dyurgerov, M. B., & Meier, M. F. (2005). *Glaciers and the changing earth system: A 2004 Snapshot*. Retrieved from University of Colorado, USA: www.instaar.colorado.edu

Fathizad, H., Rostami, N., & Faramarzi, M. (2015). Detection and prediction of land cover changes using Markov chain model in semi-arid rangeland in western Iran. *Environmental Monitoring and Assessment, 187*(10), 629. doi:10.1007/s10661-015-4805-y

Gao, J. (2017). *Downscaling global spatial population projections from 1/8-degree to 1-km grid cells*. Retrieved from https://opensky.ucar.edu

Gibson, L., Münch, Z., Palmer, A., & Mantel, S. (2018). Future land cover change scenarios in South African grasslands - implications of altered biophysical drivers on land management. *Heliyon, 4*(7), e00693-e00693. doi:10.1016/j.heliyon.2018.e00693

Gupta, N., Jethoo, A. s., & Gupta, S. (2015). Rainfall and surface water resources of Rajasthan State, India. *Water Policy, 18*, wp2015033. doi:10.2166/wp.2015.033

Hamad, R., Balzter, H., & Kolo, K. (2018). Predicting land use/land cover changes using a CA-Markov model under two different scenarios. *Sustainability, 10*(10), 3421. doi:10.3390/su10103421

IPCC. (2018). *Global warming of 1.5°C*. Retrieved from Intergovernmental Panel on Climate Change: www.ipcc.ch/sr15

Jain, S. K., Goswami, A., & Saraf, A. K. (2008). Determination of land surface temperature and its lapse rate in the Satluj River basin using NOAA data. *International Journal of Remote Sensing, 29*(11), 3091-3103. doi:10.1080/01431160701468992

Jones, B., & O'Neill, B. C. (2016). Spatially explicit global population scenarios consistent with the Shared Socioeconomic Pathways. *Environmental Research Letters, 11*(084003). doi:10.1088/1748-9326/11/8/084003

Kattelmann, R. (1987). Uncertainty in assessing Himalayan water resources. *Mountain Research and Development, 7*(3), 279-286. doi:10.2307/3673206

Kaur, B., Sidhu, R. s., & Vatta, K. (2010). Optimal crop plans for sustainable water use in Punjab. *Agricultural Economics Research Review, 23*, 273-284.

Kou, L., Li, X., Lin, J., & Kang, J. (2018). Simulation of urban water resources in Xiamen based on a WEAP model. *Water, 10*(6), 732. doi:10.3390/w10060732

Kulkarni, A., & Karyakarte, Y. (2014). Observed changes in Himalayan glaciers. *Current science, 106*, 237-244.

Kumar, V., Singh, P., & Singh, V. (2007). Snow and glacier melt contribution in the Beas River at Pandoh Dam, Himachal Pradesh, India. *Hydrological Sciences Journal, 52*(2), 376-388. doi:10.1623/hysj.52.2.376

Lenderink, G., Buishand, A., & van Deursen, W. (2007). Estimates of future discharges of the river Rhine using two scenario methodologies: direct versus delta approach. *Hydrol. Earth Syst. Sci., 11*(3), 1145-1159. doi:10.5194/hess-11-1145-2007

Liping, C., Yujun, S., & Saeed, S. (2018). Monitoring and predicting land use and land cover changes using remote sensing and GIS techniques—A case study of a hilly area, Jiangle, China. *PLOS ONE, 13*(7), e0200493. doi:10.1371/journal.pone.0200493

Marko, K., Zulkarnain, F., & Kusratmoko, E. (2016). Coupling of Markov chains and cellular automata spatial models to predict land cover changes (case study: upper Ci Leungsi catchment area). *IOP Conference Series: Earth and Environmental Science, 47*, 012032. doi:10.1088/1755-1315/47/1/012032

Momblanch, A., Papadimitriou, L., Jain, S. K., Kulkarni, A., Ojha, C. S. P., Adeloye, A. J., & Holman, I. P. (2019). Untangling the water-food-energy-environment nexus for global change adaptation in a complex Himalayan water resource system. *Science of The Total Environment, 655*, 35-47. doi:10.1016/j.scitotenv.2018.11.045

Monserud, R. A., & Leemans, R. (1992). Comparing global vegetation maps with the Kappa statistic. *Ecological Modelling, 62*(4), 275-293. doi:10.1016/0304-3800(92)90003-W

NASA. (2018). Data to information. Retrieved from www.science.nasa.gov/data-information

Nash, J. E., & Sutcliffe, J. V. (1970). River flow forecasting through conceptual models part I — A discussion of principles. *Journal of Hydrology, 10*(3), 282-290. doi:10.1016/0022-1694(70)90255-6

Pontius, R. (2000). Quantification error versus location error in comparison of categorical maps. *Photogrammetric Engineering & Remote Sensing, 66*, 1011-1016.

Pontius, R. (2002). Statistical methods to partition effects of quantity and location during comparison of categorical maps at multiple resolutions. *Photogrammetric Engineering and Remote Sensing, 68*.

Rajeevan, U., & Mishra, B. K. (2020). Sustainable management of the groundwater resource of Jaffna, Sri Lanka with the participation of households: Insights from a study on household water consumption and management. *Groundwater for Sustainable Development, 10*, 100280. doi:10.1016/j.gsd.2019.100280

Rawat, S., Lahari, S., & Gosain, A. (2018). Integrated Water Resource Assessment of Irrigation System of Haryana. *Agricultural Sciences, 09*, 489-510. doi:10.4236/as.2018.94034

Sawatpru, K., & Konyai, S. (2016). Hydrological drought frequency analysis of the Yom River, Thailand. *KKU Engineering Journal, 42*, 100-107.

Shivakoti, G., Febriamansyah, R., Yonariza, Y., & Ullah, R. (2016). *Redefining Diversity and Dynamics of Natural Resources Management in Asia, Volume 4: The Reciprocal Relationship between Governance of Natural Resources and Socio-Ecological Systems Dynamics in West Sumatra Indonesia*: Elsevier Science.

Sieber, J., & Purkey, D. (2011). *WEAP, water evaluation and planning system*. Retrieved from U.S. Center, Somerville, USA: https://www.weap21.org

Singh, S., Reddy, V. R., Batchelor, C., Marothia, D. K., James, A. J., & Rathore, M. S. (2013). *Regulating water demand and use in Rajasthan*. Retrieved from European Union: www.eeas.europa.eu

Sridharan, V., Pereira Ramos, E., Zepeda, E., Boehlert, B., Shivakumar, A., Taliotis, C., & Howells, M. (2019). The Impact of Climate Change on Crop Production in Uganda—An Integrated Systems Assessment with Water and Energy Implications. *11*(9), 1805.

UCLouvain. (2017). ESA Climate Change Initiative - Land Cover. Retrieved from http://maps.elie.ucl.ac.be/CCI/viewer/download.php

UN. (2019). *World population prospects 2019: highlights*. Retrieved from New York: www.un.org

Wang, X., Pang, G., Yang, M., & Zhao, G. (2017). Evaluation of climate on the Tibetan Plateau using ERA-Interim reanalysis and gridded observations during the period 1979–2012. *Quaternary International*, *444*, 76-86. doi:10.1016/j.quaint.2016.12.041

WaterAid-India. (2005). *Drinking water and sanitation status in India*. Retrieved from WaterAid India: www.wateraidindia.in

Yates, D., Purkey, D., Sieber, J., Huber-Lee, A., & Galbraith, H. (2005). WEAP21—A Demand-, Priority-, and Preference-Driven Water Planning Model. *Water International*, *30*(4), 501-512. doi:10.1080/02508060508691894

You, Q., Kang, S., Aguilar, E., & Yan, Y. (2008). Changes in daily climate extremes in the eastern and central Tibetan Plateau during 1961–2005. *113*(D7). doi:10.1029/2007jd009389